
Protein stabilization by specific binding of guanidinium to a functional arginine-binding surface on an SH3 domain

ARASH ZARRINE-AFSAR,¹ ANTHONY MITTERMAIER,¹ LEWIS E. KAY,^{1,2,3}
AND ALAN R. DAVIDSON^{1,2}

Departments of ¹Biochemistry, ²Molecular and Medical Genetics, and ³Chemistry, University of Toronto, Toronto, Ontario, M5S-1A8, Canada

(RECEIVED September 1, 2005; FINAL REVISION September 1, 2005; ACCEPTED October 11, 2005)

Abstract

Guanidinium hydrochloride (GuHCl) at low concentrations significantly stabilizes the Fyn SH3 domain. In this work, we have demonstrated that this stabilizing effect is manifested through a dramatic (five- to sixfold) decrease in the unfolding rate of the domain with the folding rate being affected minimally. This behavior contrasts to the effect of NaCl, which stabilizes this domain by accelerating the folding rate. These data imply that the stabilizing effect of GuHCl is not predominantly ionic in nature. Through NMR studies, we have identified a specific binding site for guanidinium, and we have determined a dissociation constant of 90 mM for this interaction. The guanidinium-binding site overlaps with a functionally important arginine-binding pocket on the domain surface, and we have shown that GuHCl is a specific inhibitor of the peptide-binding activity of the domain. A different SH3 domain possessing a similar arginine-binding pocket is also thermodynamically stabilized by GuHCl. These data suggest that many proteins that normally interact with arginine-containing ligands may also be able to specifically interact with guanidinium. Thus, some caution should be used when using GuHCl as a denaturant in protein folding studies. Since arginine-mediated interactions are often important in the energetics of protein–protein interactions, our observations could be relevant for the design of small molecule inhibitors of protein–protein interactions.

Keywords: SH3 domain; protein folding kinetics; guanidinium-induced protein stabilization; peptide binding; arginine–protein interaction; specific guanidinium binding

A multitude of experimental studies have investigated the thermodynamic stability and folding kinetics of proteins. In the majority of these studies, chemical denaturants, generally urea or guanidine hydrochloride (GuHCl), have been utilized to induce protein unfolding. Despite the routine use of chemical denaturants in these studies, the mechanisms by which these agents affect protein stability are still not fully understood (Schellman 2002).

The effects of GuHCl on protein stability are particularly complicated due to its ionic character. Ions can either bind to the folded or unfolded states of proteins or influence stability through “screening” coulombic interactions, the Hofmeister effect, or changing the structure of the solvent (for a recent review, see Collins 2004). Thus, GuHCl can modulate protein stability through mechanisms related to both its denaturant and ionic properties. Although GuHCl is thought of primarily as a denaturant, there have been many cases reported where low concentrations of GuHCl actually stabilize proteins (Mayr and Schmid 1993; Monera et al. 1994; Makhatadze et al. 1998; Bhuyan 2002). In the majority of these cases, it has been shown that the ionic nature of

Reprint requests to: Alan R. Davidson, Department of Molecular and Medical Genetics, University of Toronto, Toronto, Ontario M5S-1A8, Canada; e-mail alan.davidson@utoronto.ca; fax (416) 978-6885.

Article and publication are at <http://www.proteinscience.org/cgi/doi/10.1110/ps.051829106>.

GuHCl is the main factor in its stabilizing effect (Monera et al. 1994; Makhatadze et al. 1998). However, some studies have suggested that GuHCl may cause protein stabilization in a more specific manner (Mayr and Schmid 1993). Solution of a crystal structure of Ribonuclease A in GuHCl demonstrated direct binding of this compound to the folded state of the enzyme, resulting in a decrease in temperature factors (Dunbar et al. 1997). However, it was observed that guanidine bound to sites comprised of various amino acid residues with no obvious sequence or structural similarity among these sites detected. Guanidinium has been recently shown to be able to mimic the interactions mediated by the guanidino ($\text{H}_2\text{N}-\text{CNH}-\text{NH}_2$)⁺ moiety of an arginine side chain and restabilize a T4 Lysozyme variant with an arginine to alanine mutation (Yousef et al. 2004).

In a previous study performed in our laboratory examining the thermodynamic stabilities of several site-directed mutants of the SH3 domain of the Fyn tyrosine kinase, we found that the use of GuHCl as a denaturant in unfolding experiments resulted in measured unfolding free energy (ΔG_u) values that were higher by ~ 1.1 kcal/mol compared with those obtained using urea-induced unfolding experiments or NMR spin relaxation dispersion spectroscopy in the absence of denaturants (Maxwell and Davidson 1998; Northey et al. 2002; Di Nardo et al. 2004). Our goal in the studies presented here is to elucidate the mechanism by which GuHCl stabilizes the

Fyn SH3 domain. We have used folding kinetics studies, functional assays, mutagenesis, and NMR spectroscopy to systematically investigate the effects of GuHCl on the structure and stability of this domain, and we demonstrate the existence of a specific binding site for guanidinium on the surface of this protein.

Results and Discussion

GuHCl stabilizes the Fyn SH3 domain by slowing its unfolding rate

To obtain insights into the mechanism of stabilization by GuHCl of the Fyn SH3 domain, the folding (k_f) and unfolding (k_u) rates of a urea-denatured Fyn SH3 domain in the presence of low concentrations of GuHCl or NaCl were measured and are reported in Table 1. Since the complete unfolding of the wild-type Fyn SH3 domain requires nearly saturated solutions of urea, the unfolding arm of the chevron plot of this domain measured in urea is quite short, leading to larger than normal errors in determination of the unfolding rate (k_u) of this protein and its dependence on urea concentration (m_{k_u}) (Fig. 1; Table 1). To obtain more accurate measurements of k_u values, we also used a destabilized mutant, R40N, with a $\Delta\Delta G_u$ value of 2.61 kcal/mol with respect to wild type. The transition midpoint of urea denaturation of this mutant was shifted to a lower concentration of urea so that

Table 1. The effect of GuHCl and NaCl on folding kinetics and thermodynamic stability of urea-denatured Fyn SH3 domain

	k_f sec ⁻¹	$m_{k_f}^a$	k_u sec ⁻¹	$m_{k_u}^a$	ΔG_u^b kcal/mol
Fyn WT [GuHCl] (M)					
0	87.19 ± 4.61	0.82 ± 0.01	0.015 ± 0.009	0.40 ± 0.07	5.13 ± 0.30
0.2	81.40 ± 4.90	0.82 ± 0.02	0.004 ± 0.005	0.55 ± 0.14	5.83 ± 0.50
0.4	68.98 ± 5.40	0.81 ± 0.02	0.002 ± 0.003	0.63 ± 0.19	6.12 ± 0.70
0.6	55.90 ± 4.80	0.81 ± 0.03	0.009 ± 0.012	0.45 ± 0.20	5.19 ± 0.70
Fyn R40N [GuHCl] (M)					
0	5.46 ± 0.50	1.01 ± 0.06	0.076 ± 0.019	0.35 ± 0.04	2.52 ± 0.08
0.2	5.04 ± 0.50	0.95 ± 0.05	0.027 ± 0.009	0.50 ± 0.05	3.10 ± 0.12
0.4	3.76 ± 0.20	0.92 ± 0.04	0.031 ± 0.008	0.43 ± 0.04	2.84 ± 0.12
0.6	3.12 ± 0.16	0.98 ± 0.04	0.050 ± 0.010	0.32 ± 0.03	2.44 ± 0.08
0.8	2.07 ± 0.16	1.02 ± 0.07	0.063 ± 0.015	0.28 ± 0.04	2.06 ± 0.08
1.0	1.27 ± 0.11	0.99 ± 0.10	0.064 ± 0.018	0.30 ± 0.05	1.77 ± 0.10
Fyn R40N [NaCl] (M)					
0	5.46 ± 0.50	1.01 ± 0.06	0.076 ± 0.019	0.35 ± 0.04	2.52 ± 0.08
0.2	11.12 ± 1.27	1.09 ± 0.08	0.073 ± 0.020	0.26 ± 0.05	2.70 ± 0.12
0.4	15.28 ± 0.66	1.06 ± 0.03	0.064 ± 0.013	0.24 ± 0.03	3.24 ± 0.12
0.6	24.70 ± 1.60	1.14 ± 0.04	0.087 ± 0.047	0.17 ± 0.08	3.44 ± 0.08

Errors reported for k_f , k_u , m_{k_f} , and m_{k_u} are fitting errors. Errors reported for ΔG_u are by error propagation as described in Materials and Methods.

^a m_{k_f} and m_{k_u} are the dependence of $\ln(k_f)$ and $\ln(k_u)$, respectively, on the concentration of urea.

^b $\Delta G_u = -RT \ln(k_u/k_f)$.

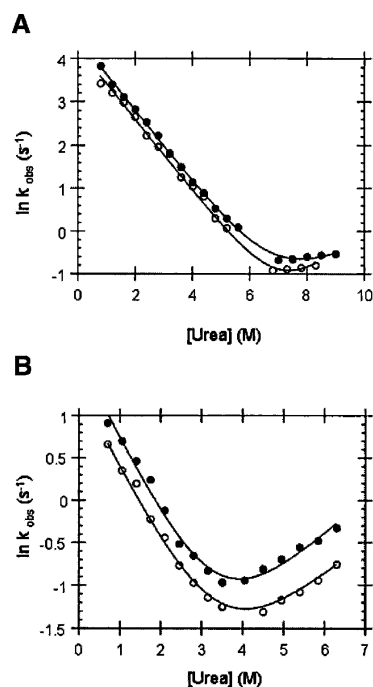


Figure 1. Chevron plots of (A) wild-type Fyn SH3 domain and (B) its R40N mutant in 0.4 M GuHCl. (●) Chevron plots in the absence of GuHCl.

more data points could be collected along the unfolding arm of the chevron plot. For both the wild type and R40N mutant, it can be seen that GuHCl is indeed highly stabilizing at low concentrations with free energy of unfolding (ΔG_u) of the wild-type domain increased by 1 kcal/mol in 0.4 M GuHCl and that of the R40N mutant increased by 0.6 kcal/mol at 0.2 M GuHCl (Table 1). It is clear that the stabilizing effect of GuHCl on this domain is manifested exclusively through slowing of the unfolding rate. For example, at 0.4 M GuHCl, the unfolding rate of the wild-type domain is slowed by 6.5-fold, while the folding rate is affected very little. The R40N mutant is stabilized in the same manner. At concentrations greater than 0.4 M, GuHCl displays a net destabilizing effect, such that the change in the free energy of unfolding (ΔG_u) of the R40N mutant assumes a strong linear relationship ($r = 0.99$) with GuHCl concentration (plot not shown). The slope of the best-fit line (1.71 kcal/mol.M) obtained using the R40N data is almost identical to the previously reported “ m_{eq} value” (1.73 kcal/mol.M) for the Fyn SH3 domain (Maxwell and Davidson 1998).

To determine whether the stabilizing effect of GuHCl was due simply to its ionic character, we compared the stabilizing effect of this compound to that of NaCl. We have reported results for only the R40N mutant here mainly because of the difficulty associated with accurate measurements of the unfolding rate (k_u) of the wild-type protein as described above. In addition, the wild-type

protein folded at such a fast rate in high NaCl that it was difficult to measure accurately. The folding rate of the Fyn R40N mutant progressively increased in the presence of increasing concentrations of salt such that a plot of the natural logarithm of the folding rate ($\ln k_f$) assumes a strong linear dependence ($r = 0.98$) on the square root of the ionic strength ($M^{1/2}$) of the NaCl concentration (plot not shown). Unfolding rates, on the other hand, essentially remained constant upon increasing salt concentration (see Table 1). In a recent study, a similar behavior for salt-mediated stabilization of the Fyn SH3 domain was observed (de Los Rios and Plaxco 2005). This behavior, where NaCl stabilizes predominantly by accelerating the folding rate, is a complete contrast to the response of the folding kinetics of the Fyn SH3 domain to increasing concentrations of GuHCl. These data imply that the mechanism of stabilization by GuHCl of this domain is not primarily ionic in nature.

The deceleration of the unfolding rate in the presence of GuHCl was accompanied by no drastic change in the folding rate, which suggests that guanidinium exclusively interacts with the native state of this protein. Consistent with this notion, the m_{kf} values remain unaltered upon increasing the concentrations of GuHCl (Table 1), whereas the m_{ku} values increase with increasing overall stability (ΔG_u). As illustrated in Figure 2, the strong correlation ($r = 0.99$ for wild type and $r = 0.92$ for R40N) between m_{ku} and ΔG_u argues for exclusive binding of guanidinium to the native state of the Fyn SH3 domain. Since the m_{ku} value is believed to be proportional to the difference in the exposed surface area between the native state and the folding transition state (Sanchez and Kiefhaber 2003), these results suggest that guanidinium binding buries part of the surface of the native state. Thus, a relatively larger surface area would become solvent exposed upon unfolding to the transition state of the guanidinium-bound Fyn SH3 domain. In addition, the lack of change of the m_{kf} value suggests that GuHCl does not preferentially interact with either the unfolded or the folding transition state of this protein.

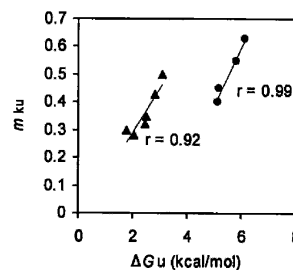


Figure 2. The correlation between ΔG_u and kinetic m_{ku} values for the wild-type Fyn SH3 domain (●) and the R40N mutant (▲) at different concentrations of GuHCl. The ΔG_u values plotted were determined at the GuHCl concentrations shown in Table 1.

NMR peak shift analysis reveals the GuHCl binding site and allows for determination of its binding affinity

To explore the possibility of specific guanidinium binding to the folded state of the Fyn SH3 domain, we collected ^{15}N - ^1H HSQC correlation spectra (Kay et al. 1992) of this protein in the presence of varying concentrations of GuHCl ranging from 0 to 0.85 M. As shown in Figure 3A, most amide peak positions are unaffected by the addition of GuHCl; however, the ^1H and ^{15}N chemical shifts of several residues exhibit dramatic changes. Notably, these peaks do not shift significantly in response to the addition of either 2 M urea or 1 M NaCl, as illustrated in Figure 3B. This suggests that the effect of GuHCl on the ^{15}N - ^1H HSQC spectrum of the Fyn SH3 domain is caused by a specific interaction and is not simply due to the ionic or denaturant properties of this compound.

Little line-broadening is evident upon GuHCl addition, even for those peaks with the greatest chemical-shift changes, indicating that exchange between guanidinium-bound and unbound states is fast on the NMR chemical shift timescale. Under these conditions, the shift in peak position relative to the 0 M GuHCl spectrum is directly proportional to the fraction of the bound state, assuming a two-state binding model. We have used data for residues whose amide resonances change by more than one peak width to estimate the fraction of bound protein as a function of GuHCl concentration, as well as the dissociation constant (K_d) for guanidinium binding on a per-residue basis. The fraction of bound protein is plotted as a function of GuHCl concentration for several residues in Figure 4, together with best-fit hyperbolic curves. Values of K_d obtained for different peaks are in good agreement with an error-weighted mean of 90 ± 0.5 mM. Individual estimates for strongly shifting residues A12, R13, T14, E15, D17, and Y49 are within 40 mM of the mean value. This estimate of a K_d value of 90 mM for the Fyn SH3 domain:GuHCl interaction is 18-fold lower than the previously reported K_d value of 1.6 M for the nonspecific interaction between proteins or peptides and GuHCl (Makhatadze and Privalov 1992; Makhatadze 1999; Moglich et al. 2005).

The magnitudes of peak shifts of residues that interact with guanidinium are color coded on the crystal structure of the Fyn SH3 domain in Figure 3C. It is clear that the largest changes in chemical shift are obtained for residues in the RT-Src loop and for residue Y49 in the fourth β strand. Interestingly, these residues are part of a conserved functional surface on SH3 domains that is often involved in binding to the side chain of a conserved arginine residue found in many SH3 target peptides. For example, the structure of a complex between the c-Src tyrosine kinase SH3 domain and the phage display-derived Vs12 peptide ligand (Feng et al. 1995) reveals that the guanidino moiety

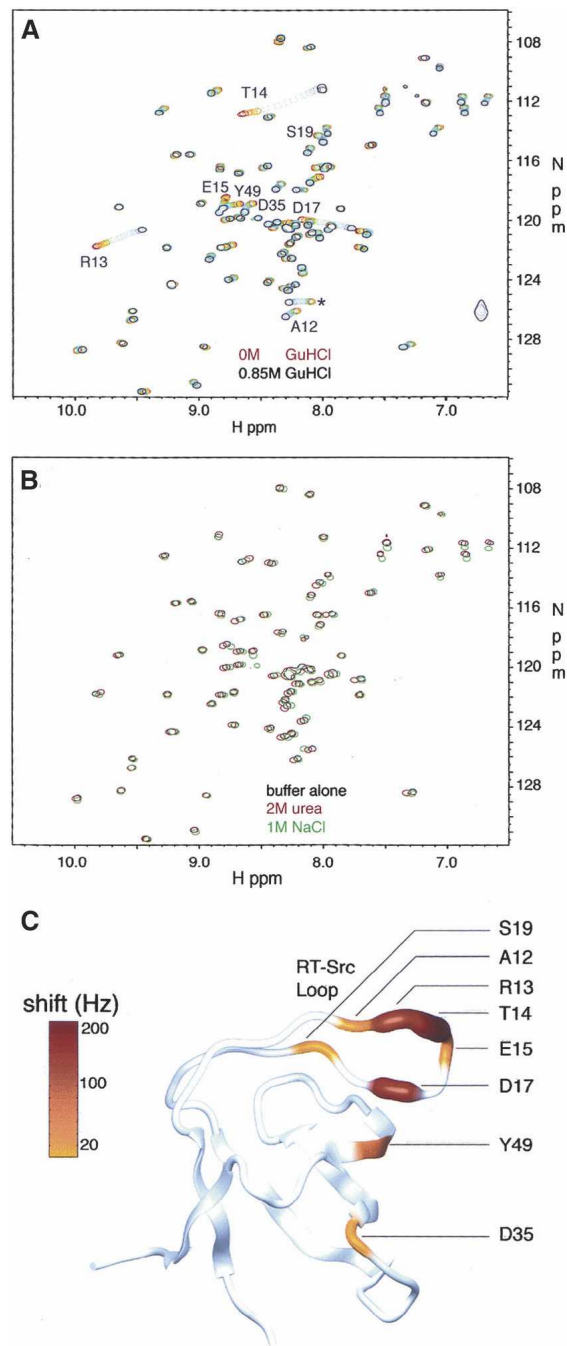


Figure 3. Overlays of ^{15}N - ^1H correlation maps collected for wild-type Fyn SH3 domain samples containing (A) 0–0.85 M GuHCl and (B) 2 M urea or 1 M NaCl. The peak marked with an asterisk in A corresponds to a residue in the C-terminal 6-his tag region of the construct that shifted significantly upon GuHCl addition. Fitting the data from this peak yielded a K_d value of 560 ± 70 mM. This K_d value is only threefold different from that reported for the nonspecific protein:GuHCl interactions and is unlikely to report on a specific interaction between the 6-his tag and GuHCl. (C) Magnitude of total baseline-corrected peak shifts ($\Delta\Omega = [\Delta\Omega_{\text{H}}^2 + \Delta\Omega_{\text{N}}^2]^{1/2}$), color coded on a ribbon-representation of the Fyn SH3 domain (generated using the coordinates of the X-ray crystal structure [Noble et al. 1993] and the program MOLMOL [Koradi et al. 1996]).

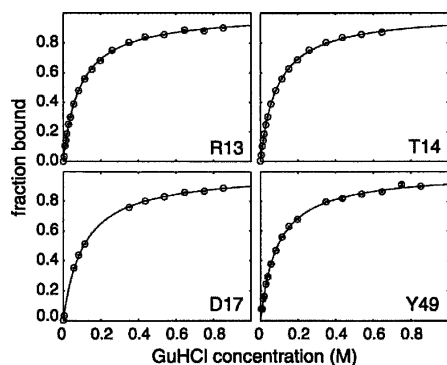


Figure 4. The guanidinium binding curves determined from NMR peak shift analysis. The fraction of protein bound is plotted as a function of GuHCl concentration with best-fit curves calculated according to Equation 2. Values were obtained from analyses of shifts in peak position in the ^1H dimension. Results shown are for four different residues as indicated in the figure.

of the target peptide arginine at the P_{-3} position (see Fig. 5C for position nomenclature) interacts with the RT-Src loop by forming hydrogen bonds with T14, T16, and D17 side chains (Fig. 5A). Since the Fyn SH3 domain also binds arginine-containing peptides, including Vsl12 (Rickles et al. 1995), and its sequence is 75% identical to that of the Src SH3 domain, it is likely that the same regions of this protein contact the conserved arginine side chain of target peptides. It is significant that both guanidinium and the arginine side chains contain a guanidino ($\text{H}_2\text{N}-\text{CNH}-\text{NH}_2$) $^+$ moiety. Thus, related interactions to those between the SH3 domain and the target-peptide arginine side chain may also stabilize a complex with guanidinium.

GuHCl inhibits the peptide-binding activity of the Fyn SH3 domain

To directly demonstrate the binding of guanidinium to the site revealed by NMR peak shift analysis we took advantage of the overlap that existed between the proposed guanidinium-binding pocket and the binding site for the natural SH3 target peptide and measured the affinity of the Fyn SH3 domain for its target peptide in the presence of varying concentrations of GuHCl and arginine. As illustrated in Figure 6, increasing the concentration of GuHCl or arginine significantly decreased the affinity of the wild-type Fyn SH3 domain for its phage-display target peptide Vsl12. At 0.4 M GuHCl, the affinity of the wild-type Fyn SH3 domain for the Vsl12 peptide decreased 25-fold compared with the affinity in the absence of GuHCl. Urea at 0.8 M concentration and NaCl at 0.4 M, on the other hand, had no significant effects on the affinity, suggesting that the denaturant and the ionic properties of GuHCl play no role in its competition with target peptide for binding to the Fyn SH3 domain (data not

shown). These observations are also consistent with NMR results suggesting no specific binding to the folded state of the Fyn SH3 domain of urea or NaCl.

In Figure 7, we compare the efficacy on an equimolar basis of GuHCl and arginine in displacing target peptide. A plot of target K_d in corresponding concentrations of GuHCl and arginine is linear ($r = 0.98$). The excellent linear correlation of this fit supports the results of the NMR experiments, demonstrating that guanidinium utilizes the arginine-binding pocket on the surface of the Fyn SH3 domain for binding. Interestingly, the slope of the best-fit line ($K_d^{\text{Arg}} = 2.3 \cdot K_d^{\text{GuHCl}}$) shows that arginine is a more potent competitor of the target peptide in binding to the Fyn SH3 domain. In the structure of the Src SH3 domain in complex with the Vsl12 peptide ligand (Feng et al. 1995), the aliphatic methylene groups of the arginine side chain in the target peptide are packed against side-chain atoms of W36 (Fig. 5B). The lack of aliphatic elements in guanidinium may explain its lower affinity for the arginine-binding pocket. Taking the above observations into consideration, we conclude that the displacement of target peptide by GuHCl is a direct result of the specific binding of guanidinium to the arginine-binding pocket of the Fyn SH3 domain.

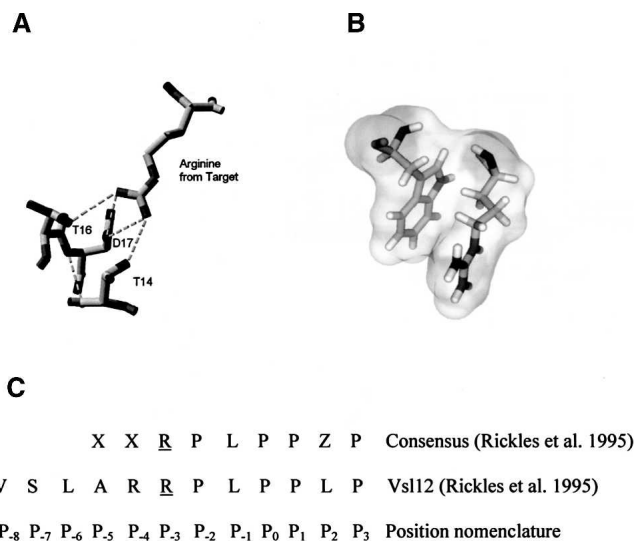


Figure 5. The interactions of the conserved arginine in SH3 domain ligands. (A) The guanidino moiety of the arginine side chain is involved in forming hydrogen bonds with the side chains of T14, T16, and D17 in the Src SH3 domain. (B) The aliphatic moiety of the arginine side chain donated by the target is also closely stacked against the side chain of W36. Figures were generated using the PDB file 1QWF (Feng et al. 1995) and the program PyMOL (DeLano Scientific). (C) The consensus sequence of phage display targets that have affinity for the Fyn SH3 domain is given along with the sequence of the Vsl12 ligand and the position nomenclature. The symbol X in the consensus sequence is any residue, and Z denotes hydrophobic residues. The conserved arginine residue at the P_{-3} position is underlined.

Upon guanidinium binding, the T14 residue in the arginine-binding pocket exhibited the greatest amide proton resonance frequency shift ~ 200 Hz. To experimentally test whether T14 is critical for binding of guanidinium, we analyzed the binding of the Vsl12 target peptide to the T14R mutant in the presence of increasing concentrations of GuHCl ranging from 0 to 0.4 M. The T14R mutant lacking the critical T14 residue binds target peptide with a K_d value of $8.83 \pm 0.48 \mu\text{M}$, about 40-fold weaker than wild type. However, as illustrated in Figure 6, the addition of GuHCl has little effect on the affinity of T14R for its target peptide. Consistent with the results of the NMR experiments, these observations argue for a critical role of T14 in the binding of guanidinium, and confirm that the interaction between the Fyn SH3 domain and guanidinium is highly specific.

Does GuHCl stabilize other SH3 domains?

To address the question of whether stabilization by GuHCl might be a general feature of proteins that interact with arginine, we examined the ability of GuHCl to stabilize two other SH3 domains, one from the yeast Actin Binding Protein 1 (Abp1) protein and the other from the yeast Sho1 protein. As a simple means to test the stabilizing effect of GuHCl on these domains, we performed temperature-induced unfolding experiments in varying amounts of GuHCl. As expected, the wild-type Fyn SH3 domain exhibited an increase in the midpoint of its temperature-induced unfolding transition (T_m) in the presence of low concentrations of GuHCl, which was maximal at 0.2 M GuHCl, where the T_m was

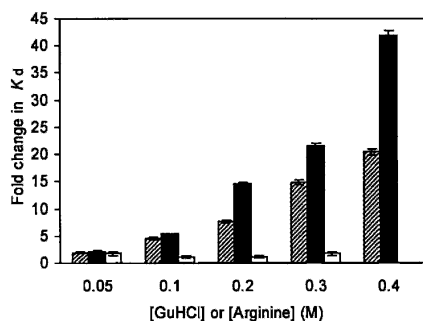


Figure 6. The effect of GuHCl on the affinity of the wild-type Fyn SH3 domain (hatched bars) and the T14R mutant (open bars) for the Vsl12 target peptide. Black bars indicate the effect of arginine on the affinity of the wild-type Fyn SH3 domain for this ligand. The reported “fold change” in K_d was calculated by normalizing the K_d value obtained at any concentration of GuHCl or arginine to the value obtained in the absence of GuHCl or arginine. Depicted error bars in each case indicate fitting errors. The K_d of T14R in 0.4 M GuHCl was not determined. The interaction between wild-type Fyn SH3 domain and target peptide in 0 M GuHCl has a K_d value of $0.22 \pm 0.01 \mu\text{M}$.

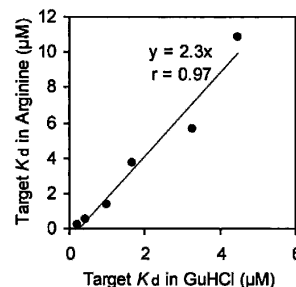


Figure 7. The influence of arginine and guanidinium binding on the affinity of the SH3 domain for its target peptide. Affinity of the wild-type Fyn SH3 domain for target peptide is plotted at corresponding concentrations of arginine and GuHCl.

increased by 3.6°C (Fig. 8). The Sho1 SH3 domain exhibited an even greater degree of stabilization in the presence of GuHCl with a T_m increase of more than 7°C at 0.1 M GuHCl. In contrast, the Abp1 SH3 domain did not exhibit an increase in T_m at any concentration of GuHCl. Since the Sho1 SH3 domain has been shown to bind strongly to target peptides possessing arginine at the P_{-3} position (Marles et al. 2004), the stabilization of this domain by GuHCl is not surprising. On the other hand, the Abp1 SH3 domain binds tightly to a different class of peptide ligands containing lysine at the P_{-3} position (Rath and Davidson 2000; Zarrinpar et al. 2004), and this domain has never been directly shown to tightly bind peptides containing arginine at the P_{-3} position⁴. These data suggest that the ability of SH3 domains to be stabilized by GuHCl correlates with their ability to bind to peptides possessing arginine at the P_{-3} position.

Conclusions

We have demonstrated, for the first time, the presence of a specific binding pocket for guanidinium on the surface of a protein, which overlaps with a functionally important arginine-binding surface. Our data show that guanidinium binding to the Fyn SH3 domain results in increased thermodynamic stability and specific inhibition of function. Another SH3 domain, which binds arginine-containing peptides, is also stabilized by GuHCl. Our results raise the possibility that any protein with an arginine-binding site may be stabilized by

⁴A study by Fazi et al. (2002), however, has suggested that the Abp1 SH3 domain may still have an affinity for peptides containing arginine at the P_{-3} position, as assessed by phage display experiments, but the affinity of these interactions has never been measured. These interactions may not be as strong as those to peptides containing lysine at the P_{-3} position.

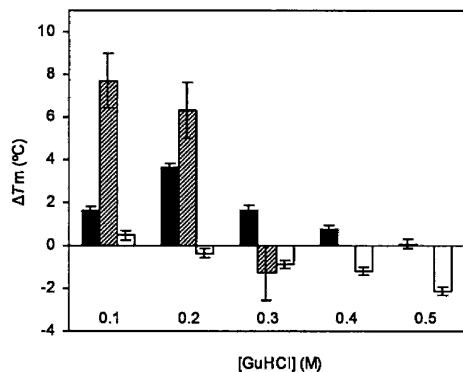


Figure 8. Influence of GuHCl on the T_m of the wild-type Fyn SH3 domain (black bars), the Sho1 SH3 domain (hatched bars), and the Abp1 SH3 domain (open bars). All of the ΔT_m values are with respect to the T_m in 0 M GuHCl. A negative ΔT_m value is indicative of destabilization. Error bars indicate uncertainties associated with fitting denaturation profiles to the appropriate equations as described in Materials and Methods. The Sho1 SH3 domain did not exhibit cooperative unfolding at GuHCl concentration of 0.4 M or higher. The wild-type Fyn, Abp1, and Sho1 SH3 domains in 0 M GuHCl have T_m values of 76.9 ± 0.11 , 53.43 ± 0.20 , and 47.75 ± 1.37 ($^{\circ}\text{C}$), respectively.

GuHCl. Since arginine is one of the three most common amino acids that are both present and energetically important within protein–protein interaction interfaces (Jones and Thornton 1996; Bogan and Thorn 1998), many proteins must possess arginine-binding pockets on their surfaces. Thus, the phenomenon of specific protein stabilization by guanidinium may be considerably more widespread than has been previously recognized. This observation should provide a note of caution for investigators using GuHCl as a denaturant in quantitative studies of protein folding and stability. On the other hand, the knowledge that many protein–protein interaction interfaces will specifically bind to guanidinium could provide a new starting point for the rational design of small molecule inhibitors of these interactions.

Materials and methods

Chemicals

Optical grade solutions of 8 M GuHCl were purchased from Pierce Biotechnology. Bioshop Canada was the provider of biotechnology grade urea and NaCl used in this study.

Mutagenesis and protein purification

All of the proteins and protein variants used in this study were expressed as C-terminal hexahistidine fusions in *Escherichia coli* strain BI21* (DE3). Recombinant proteins were purified using nickel affinity chromatography under denaturing

conditions as described previously (Maxwell and Davidson 1998). Proteins were folded through dialysis and used as such without cleaving the hexahistidine tag. The dialysis buffer consisted of a 50 mM sodium phosphate solution (pH 7.0). Protein folding and functional assays were performed in this buffer.

Folding kinetics

Folding and unfolding rates were measured at 298 K on a Bio-Logic SFM-4 stopped-flow device equipped with a Photo Multiplier Tube (PMT) monitoring the recovery of intrinsic Trp fluorescence upon folding of urea denatured protein. Excitation was carried out at 295 nm and all of the fluorescence above 309 nm was collected. Traces were fit to appropriate single exponential functions using BioKine. At each concentration of urea, at least five separate shots of 3–5 μM protein were averaged. Assuming a linear dependence of $\ln k_{\text{obs}}$ on urea concentration, kinetic chevron plots were fit to chevron equation:

$$\ln k_{\text{obs}} = \ln k_f - (m_{\text{kf}}[\text{urea}]) + \ln k_u + (m_{\text{ku}}[\text{urea}])$$

where k_f and k_u are the folding and unfolding rates at 0 M urea and m_{kf} and m_{ku} denote the dependence of k_f and k_u on the concentration of denaturant. Fitting was performed by a least squares method using Kaleidagraph (Synergy software).

NMR spectroscopy and quantitative peak shift studies

NMR experiments were performed on 0.25 mM uniformly ^{15}N isotopically enriched protein samples containing 50 mM sodium phosphate (pH 7.0), 100 mM NaCl, 0.2 mM EDTA, and 4 mM DSS at 25°C using a Varian Inova spectrometer operating at 500 MHz ^1H frequency. GuHCl was added to final concentrations of 0, 5, 10, 15, 20, 29, 38, 57, 83, 115, 153, 198, 260, 350, 436, 538, 646, 750, and 851 mM. Spectra were processed and peak positions quantitated using the NMRPipe/NMRDraw suite of programs (Delaglio et al. 1995), referencing ^1H and ^{15}N chemical shifts relative to the ^1H methyl resonances of DSS (Wishart et al. 1995). Assignment of NMR spectra was accomplished with a ^{15}N , ^{13}C -labeled protein sample under identical buffer conditions using HNCACB (Wittekind and Mueller 1993) and TOCSY-HSQC (Montelione et al. 1992; Logan et al. 1993) pulse sequences.

Amide ^{15}N and ^1H chemical shifts showing changes greater than 0.4 or 0.08 ppm, respectively, were fit separately to the equation

$$\Omega(C) = \Omega_0 + f_B \times (\Omega_F - \Omega_0) + m \times C \quad [1]$$

where $\Omega(C)$ is the chemical shift at GuHCl concentration C , $\Omega_0 = \Omega(0)$, $\Omega_F = \Omega(\infty)$, and m is a baseline correction factor discussed below. f_B is the fraction of protein bound to GuHCl, which is given by

$$f_B = C / (C + K_d) \quad [2]$$

The parameters Ω_0 , Ω_F , m , and K_d were allowed to vary in least-squares fits of the data. The weighted mean of the dissociation constant was calculated according to

$$K = (\sum w_j K_j) / (\sum w_j), w_j = 1 / (\sigma_j^2) \quad [3]$$

where σ_j is the experimental uncertainty in the dissociation constant, K_j , calculated from a single set of ^1H or ^{15}N chemical shifts, and the sum extends over all individual K_d estimates. The uncertainty in the weighted mean was computed using a bootstrap simulation (Efron and Tibshirani 1986).

Linear baseline corrections were found to be necessary for adequate fits of experimental data. Extracted values range from $m = -0.30$ ppm/M for A12 to 0.06 ppm/M for T14 ^1H chemical shifts; in the case of ^{15}N chemical shifts, the range extends from -1.29 ppm/M for T14 to 0.39 ppm/M for D35. This linear dependence on GuHCl concentration is likely due to either slight noncooperative changes in protein conformation or very weak guanidinium binding in addition to the stronger ($K_d \approx 90$ mM) interaction.

Binding studies

Dissociation constants were measured using the changes in the intrinsic fluorescence of the Trp residue located in the target binding pocket of the Fyn SH3 domain as a probe for binding. A λ CI fusion construct of a previously characterized Vsl12 target peptide (Maxwell and Davidson 1998) was used in these studies. Fluorescence signal was collected at equilibrium on an Aviv Spectrofluorometer Model ATF 105 (Aviv Associates). After subtraction of the fluorescence contribution from target alone from that of the complex, fluorescence data were fit as described previously (Maxwell and Davidson 1998).

Temperature melts

The changes in the ellipticity (mdeg) at 220 nm were recorded at equilibrium at different temperatures on an Aviv Circular Dichroism spectrometer Model 62A DS (Aviv Associates). Sigmoidal unfolding curves were fit by nonlinear least-squares methods using the program Igor Pro to the standard equations to obtain the T_m as described previously (Maxwell and Davidson 1998).

Error analysis

The errors reported for k_{obs} , m_{KF} , m_{Ku} , K_d , and T_m are uncertainties associated with the least-squares fitting of the data to appropriate equations. Folding kinetics experiments, temperature melts, and binding assays were repeated at least twice. In all cases, the variations observed in k_{obs} , m_{KF} , m_{Ku} , K_d , and T_m parameters were $< 5\%$. Uncertainties reported for ΔG , ΔT_m are by error propagation according to the general equation:

$$u = \sqrt{\left[\left(\frac{\partial u}{\partial x} \right)^2 (dx)^2 + \left(\frac{\partial u}{\partial y} \right)^2 (dy)^2 \right]}$$

where $u = f(x, y)$ and dx and dy are the residual errors of x and y , respectively.

Acknowledgments

A.Z.-A. is supported by a doctorate Canada Graduate Scholarship (CGS) from the Natural Sciences and Engineering Research Council of Canada (NSERC). This work was supported by operating grants from the Canadian Institutes of Health Research to A.R.D. and L.E.K.

References

- Bhuyan, A.K. 2002. Protein stabilization by urea and guanidine hydrochloride. *Biochemistry* **41**: 13386–13394.
- Bogan, A.A. and Thorn, K.S. 1998. Anatomy of hot spots in protein interfaces. *J. Mol. Biol.* **280**: 1–9.
- Collins, K.D. 2004. Ions from the Hofmeister series and osmolytes: Effects on proteins in solution and in the crystallization process. *Methods* **34**: 300–311.
- de Los Rios, M.A. and Plaxco, K.W. 2005. Apparent Debye-Huckel electrostatic effects in the folding of a simple, single domain protein. *Biochemistry* **44**: 1243–1250.
- Delaglio, F., Grzesiek, S., Vuister, G.W., Zhu, G., Pfeifer, J., and Bax, A. 1995. NMRPipe: A multidimensional spectral processing system based on UNIX pipes. *J. Biomol. NMR* **6**: 277–293.
- Di Nardo, A.A., Korzhnev, D.M., Stogios, P.J., Zarrine-Afsar, A., Kay, L.E., and Davidson, A.R. 2004. Dramatic acceleration of protein folding by stabilization of a nonnative backbone conformation. *Proc. Natl. Acad. Sci.* **101**: 7954–7959.
- Dunbar, J., Yennawar, H.P., Banerjee, S., Luo, J., and Farber, G.K. 1997. The effect of denaturants on protein structure. *Protein Sci.* **6**: 1727–1733.
- Efron, B. and Tibshirani, R. 1986. Bootstrap methods for standard errors, confidence intervals and other measures of statistical accuracy. *Stat. Sci.* **1**: 54–77.
- Fazi, B., Cope, M.J., Douangamath, A., Ferracuti, S., Schirwitz, K., Zucconi, A., Drubin, D.G., Wilmanns, M., Cesareni, G., and Castagnoli, L. 2002. Unusual binding properties of the SH3 domain of the yeast actin-binding protein Abp1: Structural and functional analysis. *J. Biol. Chem.* **277**: 5290–5298.
- Feng, S., Kasahara, C., Rickles, R.J., and Schreiber, S.L. 1995. Specific interactions outside the proline-rich core of two classes of Src homology 3 ligands. *Proc. Natl. Acad. Sci.* **92**: 12408–12415.
- Jones, S. and Thornton, J.M. 1996. Principles of protein-protein interactions. *Proc. Natl. Acad. Sci.* **93**: 13–20.
- Kay, L.E., Keifer, P., and Saarinen, T. 1992. Pure absorption gradient enhanced heteronuclear single quantum correlation spectroscopy with improved sensitivity. *J. Am. Chem. Soc.* **114**: 10663–10665.
- Koradi, R., Billeter, M., and Wuthrich, K. 1996. MOLMOL: A program for display and analysis of macromolecular structures. *J. Mol. Graph.* **14**: 51–55.
- Logan, T.M., Olejniczak, E.T., Xu, R.X., and Fesik, S.W. 1993. A general method for assigning NMR spectra of denatured proteins using 3D HC(CO)NH-TOCSY triple resonance experiments. *J. Biomol. NMR* **3**: 225–231.
- Makhataдзе, G.I. 1999. Thermodynamics of protein interactions with Urea and Guanidinium Hydrochloride. *J. Phys. Chem. B* **103**: 4781–4785.
- Makhataдзе, G.I. and Privalov, P.L. 1992. Protein interactions with urea and guanidinium chloride. A calorimetric study. *J. Mol. Biol.* **226**: 491–505.
- Makhataдзе, G.I., Lopez, M.M., Richardson 3rd, J.M., and Thomas, S.T. 1998. Anion binding to the ubiquitin molecule. *Protein Sci.* **7**: 689–697.
- Marles, J.A., Dahesh, S., Haynes, J., Andrews, B.J., and Davidson, A.R. 2004. Protein-protein interaction affinity plays a crucial role in controlling the Sho1p-mediated signal transduction pathway in yeast. *Mol. Cell* **14**: 813–823.
- Maxwell, K.L. and Davidson, A.R. 1998. Mutagenesis of a buried polar interaction in an SH3 domain: Sequence conservation provides the best prediction of stability effects. *Biochemistry* **37**: 16172–16182.
- Mayr, L.M. and Schmid, F.X. 1993. Stabilization of a protein by guanidinium chloride. *Biochemistry* **32**: 7994–7998.
- Moglich, A., Krieger, F., and Kiefhaber, T. 2005. Molecular basis for the effect of urea and guanidinium chloride on the dynamics of unfolded polypeptide chains. *J. Mol. Biol.* **345**: 153–162.
- Monera, O.D., Kay, C.M., and Hodges, R.S. 1994. Protein denaturation with guanidine hydrochloride or urea provides a different estimate of stability depending on the contributions of electrostatic interactions. *Protein Sci.* **3**: 1984–1991.
- Montelione, G.T., Lyons, B.A., Emerson, S.D., and Tashiro, M. 1992. An efficient triple resonance experiment using carbon 13 isotropic mixing for determining sequence-specific resonance assignments of isotopically-enriched proteins. *J. Am. Chem. Soc.* **114**: 10974–10975.
- Noble, M.E., Musacchio, A., Saraste, M., Courtneidge, S.A., and Wierenga, R.K. 1993. Crystal structure of the SH3 domain in human Fyn; comparison of the three-dimensional structures of SH3 domains in tyrosine kinases and spectrin. *EMBO J.* **12**: 2617–2624.
- Northey, J.G., Di Nardo, A.A., and Davidson, A.R. 2002. Hydrophobic core packing in the SH3 domain folding transition state. *Nat. Struct. Biol.* **9**: 126–130.

- Rath, A. and Davidson, A.R. 2000. The design of a hyperstable mutant of the Abp1p SH3 domain by sequence alignment analysis. *Protein Sci.* **9**: 2457–2469.
- Rickles, R.J., Botfield, M.C., Zhou, X.M., Henry, P.A., Brugge, J.S., and Zoller, M.J. 1995. Phage display selection of ligand residues important for Src homology 3 domain binding specificity. *Proc. Natl. Acad. Sci.* **92**: 10909–10913.
- Sanchez, I.E. and Kiefhaber, T. 2003. Hammond behavior versus ground state effects in protein folding: Evidence for narrow free energy barriers and residual structure in unfolded states. *J. Mol. Biol.* **327**: 867–884.
- Schellman, J.A. 2002. Fifty years of solvent denaturation. *Biophys. Chem.* **96**: 91–101.
- Wishart, D.S., Bigam, C.G., Yao, J., Abildgaard, F., Dyson, H.J., Oldfield, E., Markley, J.L., and Sykes, B.D. 1995. ^1H , ^{13}C and ^{15}N chemical shift referencing in biomolecular NMR. *J. Biomol. NMR* **6**: 135–140.
- Wittekind, M. and Mueller, L. 1993. HNCACB, a high sensitivity 3D NMR experiment to correlate amide proton and nitrogen resonances with the α - and β -carbon resonances in proteins. *J. Magn. Reson. Series B* **101**: 201–205.
- Yousef, M.S., Baase, W.A., and Matthews, B.W. 2004. Use of sequence duplication to engineer a ligand-triggered, long-distance molecular switch in T4 lysozyme. *Proc. Natl. Acad. Sci.* **101**: 11583–11586.
- Zarrinpar, A., Bhattacharyya, R.P., Nittler, M.P., and Lim, W.A. 2004. Sho1 and Pbs2 act as coscaffolds linking components in the yeast high osmolarity MAP kinase pathway. *Mol. Cell* **14**: 825–832.